



## Derivation of the unified charge control model and parameter extraction procedure

Ana Isabela Araújo Cunha \*, Márcio Cherem Schneider, Carlos Galup-Montoro

*Departamento de Engenharia Elétrica, Universidade Federal de Santa Catarina, C.P. 476, CEP 88040-900, Florianópolis, SC, Brazil*

Received 10 November 1997; received in revised form 22 June 1998

---

### Abstract

This paper presents a physical derivation of the unified charge control model (UCCM) [Park C-K, Lee C-Y, Lee K, Moon B-J, Byun YH, Shur M. IEEE Trans Electron Dev 1991;ED-38:399; Lee K, Shur M, Fjeldly TA, Ytterdal T. Semiconductor device modeling for VLSI. Englewoods Cliffs: Prentice Hall, 1993.], which describes the relationship between inversion charge density and the applied voltages in the MOS transistor for any operating region. Using the UCCM and the MOSFET charge model presented in Cunha et al. [Cunha AIA, Schneider MC, Galup-Montoro C. Solid-St Electron 1995;38:1945.], we develop a MOSFET model formulated in terms of the drain current in saturation. Based on this model, a methodology for the extraction of the UCCM parameters is proposed. © 1999 Published by Elsevier Science Ltd. All rights reserved.

---

### 1. NOTATION

$C'_{\text{ox}}$  oxide capacitance per unit area ( $\text{F}/\text{m}^2$ )  
 $I_{\text{D}}$  drain current (A)  
 $I_{\text{F}}$  forward saturation current (A)  
 $i_{\text{f}}$  forward normalized current (dimensionless)  
 $I_{\text{R}}$  reverse saturation current (A)  
 $i_{\text{r}}$  reverse normalized current (dimensionless)  
 $I_{\text{S}}$  normalization current (A)  
 $L$  effective channel length (m)  
 $n$  slope factor (dimensionless)  
 $Q'_{\text{I}}$  inversion charge density ( $\text{C}/\text{m}^2$ )  
 $Q'_{\text{ID}}$  inversion charge density at drain ( $\text{C}/\text{m}^2$ )  
 $Q'_{\text{IS}}$  inversion charge density at source ( $\text{C}/\text{m}^2$ )  
 $Q'_{\text{IP}}$  inversion charge density at pinch-off ( $\text{C}/\text{m}^2$ )  
 $t_{\text{ox}}$  oxide thickness (m)  
 $V_{\text{C}}$  channel voltage = difference between the electron quasi-Fermi potential and the bulk Fermi potential (V)

$V_{\text{D}}$  drain voltage (V)  
 $V_{\text{G}}$  gate voltage (V)  
 $V_{\text{P}}$  pinch-off voltage (V)  
 $V_{\text{S}}$  source voltage (V)  
 $V_{\text{TO}}$  threshold voltage at equilibrium (V)  
 $W$  effective channel width (m)  
 $\phi_{\text{S}}$  surface potential (V)  
 $\phi_{\text{t}}$  thermal voltage (V)  
 $\gamma$  body effect factor ( $\text{V}^{1/2}$ )  
 $\mu$  carrier mobility ( $\text{m}^2/(\text{V}\cdot\text{s})$ )

### 2. Introduction

As a consequence of the trend towards shorter channel lengths and reduced supply voltages, MOS devices are expected to often operate in the moderate and weak inversion regions. In this work, we present a formal derivation of UCCM, a MOSFET model applicable to any region of inversion. We first derive a relationship between charge and applied voltages similar to UCCM. Next, we combine the relation between

---

\* Corresponding author. Permanent address: Departamento de Engenharia Elétrica da Escola Politécnica, Universidade Federal da Bahia, CEP 40210-630, Salvador, BA, Brazil. Tel.: +55-71-237-2367; fax: +55-71-237-2367.

charge and voltage and the expression for the drain current derived in [3] to obtain an  $I$ - $V$  MOSFET model. Finally, we propose a very simple procedure for extracting the parameters of the UCCM model.

### 3. Derivation of the unified charge control model

From the MOS three terminal charge balance equation [5] (p. 79) it is easy to show [3] that for constant gate-to-bulk potential ( $V_G$ )

$$\left. \frac{d\phi_s}{dV_C} \right|_{V_G} = \frac{C'_i}{C'_i + C'_b + C'_{ox}} \quad (1)$$

where  $\phi_s$  is the surface potential,  $V_C(x)$  is the difference between the quasi-Fermi potentials of electrons and holes, and  $C'_i$ ,  $C'_{ox}$ ,  $C'_b$  are the inversion, oxide and depletion capacitances per unit area, respectively.

As shown in [3], for constant gate to substrate potential, the inversion charge density can be approximated by a linear function of the surface potential

$$dQ'_I = (C'_{ox} + C'_b)d\phi_s = nC'_{ox}d\phi_s, \quad (2)$$

where  $n$  is the so-called slope factor and is slightly dependent on the gate potential through  $C'_b$ .

The substitution of the fundamental approximation of Eq. (2) into Eq. (1) leads to

$$\left. \frac{dQ'_I}{dV_C} \right|_{V_G} = \frac{(C'_{ox} + C'_b)C'_i}{C'_{ox} + C'_b + C'_i}. \quad (3)$$

Eq. (3) is equivalent to the small signal model shown in Fig. 1. In weak, moderate and not very strong inversion, the inversion capacitance can be approximated [3] by

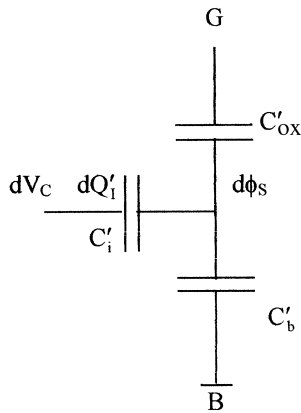


Fig. 1. Small-signal model for the three terminal MOSFET.

$$C'_i = -\frac{Q'_I}{\phi_t}. \quad (4)$$

In very strong inversion, Eq. (4) overestimates the inversion capacitance by a factor of 2, but in this region  $C'_i \gg C'_{ox}$ ,  $C'_b$  and, therefore, its exact value is not relevant to calculate the derivative in Eq. (3). Indeed, for very strong inversion, the right-hand side of Eq. (3) can be approximated by  $(C'_{ox} + C'_b)$ .

The substitution of Eq. (4) into Eq. (3) allows obtaining the following relationship between  $C'_i$  and  $V_C$

$$dQ'_I \left( \frac{1}{nC'_{ox}} - \frac{\phi_t}{Q'_I} \right) = dV_C. \quad (5)$$

Integrating Eq. (5) from an arbitrary channel potential  $V_C$  to the pinch-off voltage  $V_P$ , yields

$$\frac{Q'_{IP} - Q'_I}{nC'_{ox}} + \phi_t \ln \left( \frac{Q'_I}{Q'_{IP}} \right) = V_P - V_C, \quad (6)$$

where  $Q'_{IP}$  is the value of  $Q'_I$  at pinch-off.

Substituting into Eq. (6) the first order approximation of  $V_P$  presented in [4]

$$V_P \cong \frac{V_G - V_{T0}}{n} \quad (7)$$

gives

$$\begin{aligned} Q'_{IP} - Q'_I + nC'_{ox}\phi_t \ln \left( \frac{Q'_I}{Q'_{IP}} \right) \\ = C'_{ox}(V_G - V_{T0} - nV_C), \end{aligned} \quad (8)$$

where  $V_{T0}$  is the threshold voltage in equilibrium.

Eq. (8) is almost identical to the unified charge control model [1,2], which was first presented as an empirical result. In fact, the UCCM is based on the linear dependence of the inversion capacitance on the inversion charge, the charge-sheet approximation and the linear relationship between inversion charge density and surface potential. In Fig. 2 we compare the values of the inversion charge density calculated by either using Eq. (6) or the expression of  $Q'_I$  in terms of  $\phi_s$  from the charge-sheet approximation [5] (p. 79), with  $\phi_s$  numerically evaluated in terms of  $V_C$ . It can be readily verified that the charge-sheet model and expression (6) are almost equivalent throughout the entire inversion region of operation.

### 4. Long channel $I$ - $V$ modeling

The model presented in [3] consists of a set of expressions for the MOSFET static and dynamic characteristics. These expressions are functions of the inversion charge densities (calculated at source ( $Q'_{IS}$ ) and drain ( $Q'_{ID}$ )) and their derivatives with respect to

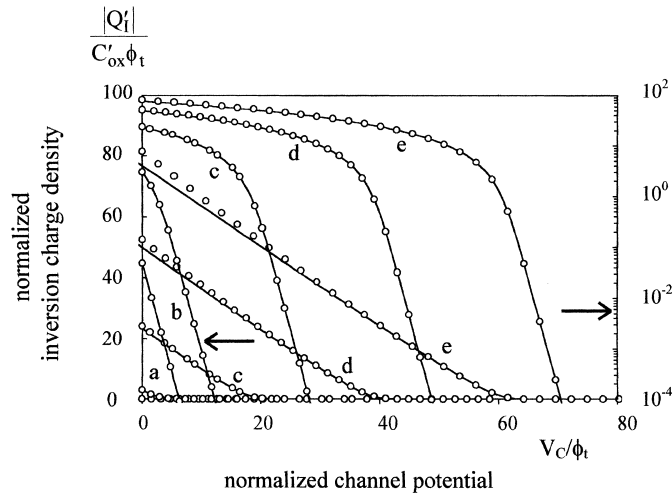


Fig. 2. Normalized inversion charge density vs. normalized channel potential calculated from: (—) expression (6) and (○) the implicit charge-sheet expression [5] (p. 79), with the surface potential numerically evaluated.  $V_G - V_{T0}$  equal to: (a)  $-5\phi_t$ , (b)  $5\phi_t$ , (c)  $30\phi_t$ , (d)  $60\phi_t$ , (e)  $90\phi_t$ .

the source and drain voltages. Combining the model in [3] with expression (6), allows one to express the MOSFET characteristics in terms of the applied gate-to-bulk ( $V_G$ ), source-to-bulk ( $V_S$ ) and drain-to-bulk ( $V_D$ ) voltages.

In [3], the MOSFET drain current is determined by substituting the basic approximation of Eq. (2) into the expression

$$I_D = \mu W \left( -Q'_I \frac{d\phi_S}{dx} + \phi_t \frac{dQ'_I}{dx} \right) \quad (9)$$

and integrating along the channel length, thus obtaining:

$$I_D = I_F - I_R \quad (10a)$$

$$I_{F(R)} = \mu n C'_{ox} \frac{W \phi_t^2}{L} \frac{1}{2} \left[ \left( \frac{Q'_{IS(D)}}{n C'_{ox} \phi_t} \right)^2 - 2 \frac{Q'_{IS(D)}}{n C'_{ox} \phi_t} \right], \quad (10b)$$

where  $\mu$  is the electron mobility,  $W$  is the channel width and  $L$  is the channel length.

The expressions of Eqs. (10a)–(b) describe the drain current of a long-channel MOS transistor as the difference between two symmetric terms: the forward saturation current  $I_F$ , which depends only on  $V_S$  and  $V_G$ , and the reverse saturation current  $I_R$ , which depends only on  $V_D$  and  $V_G$ . In forward saturation,  $I_R$  vanishes and the drain current equals  $I_F$ . Hence,  $I_F$  can be measured from the circuit shown in Fig. 3. Analogously,  $I_D$  approaches  $I_R$  in reverse saturation.

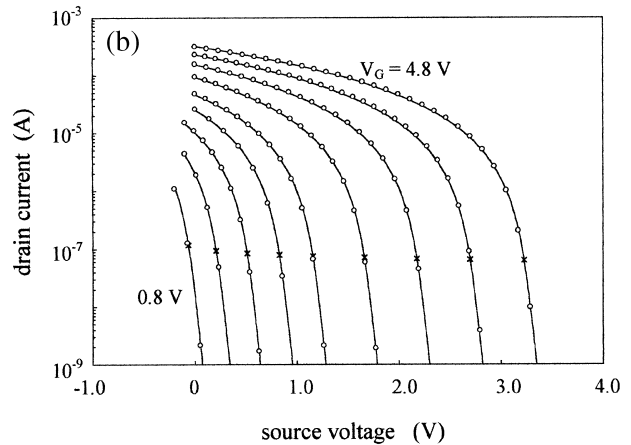
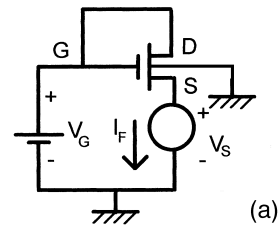


Fig. 3. (a) Circuit configuration for measuring the common-gate characteristics in saturation. (b) Common-gate characteristics in saturation of an NMOS transistor with  $t_{ox} = 280 \text{ \AA}$  and  $W = L = 25 \text{ \mu m}$  ( $V_G = 0.8, 1.2, 1.6, 2.0, 2.4, 3.0, 3.6, 4.2$  and  $4.8 \text{ V}$ ): (—) simulated curves calculated from Eq. (12); (○) measured curves; (\*) measured points corresponding to logarithmic derivative equal to  $-2/3\phi_t$  and  $V_S = V_P$  ( $i_t = 3$ ).

From Eqs. (10a)–(b), we derive the relationship between the inversion charge density calculated at each channel end and its corresponding current component ( $I_F$  or  $I_R$ )

$$-\frac{Q'_{IS(D)}}{nC'_{ox}\phi_t} = \sqrt{1+i_{f(r)}} - 1, \quad (11a)$$

where  $i_{f(r)}$  is the forward (reverse) normalized current [4] defined as

$$i_{f(r)} = \frac{I_{F(R)}}{I_S} \quad (11b)$$

and  $I_S$  is the normalization current, given by

$$I_S = \mu n C'_{ox} \frac{W\phi_t^2}{L/2} \quad (11c)$$

which is equal to the threshold current in saturation,  $I_t$ , defined in Ref. [2] (p. 311) and is four times smaller than the homonym presented in [4].

The substitution of Eq. (11a) into Eq. (6) leads to the following universal relationship between the forward (reverse) normalized current and the source (drain) normalized voltage

$$\frac{V_P - V_{S(D)}}{\phi_t} = \sqrt{1+i_{f(r)}} - \sqrt{1+i_P} + \ln\left(\frac{\sqrt{1+i_{f(r)}} - 1}{\sqrt{1+i_P} - 1}\right), \quad (12)$$

where  $i_P$  is the value of  $i_{f(r)}$  for  $V_{S(D)} = V_P$ .

Expression of Eq. (12) is independent of technology, transistor dimensions and temperature. It is noticeable

from Eq. (12) that the forward and reverse saturation characteristics ( $I_F$  vs.  $V_S$  or  $I_R$  vs.  $V_D$ ) are exactly the same.

## 5. Parameter extraction and results

The parameters of the long-channel model can be extracted using the following procedure:

1. To determine the normalization current  $I_S(V_G)$ , we measure the 'common-gate' characteristics in saturation ( $V_D = V_G$ ) for several values of  $V_G$ , as illustrated in Fig. 3. The logarithmic derivative of the forward current calculated from Eq. (12) is given by

$$\frac{\partial \ln I_F}{\partial V_S} = -\frac{2}{\phi_t(1 + \sqrt{1+i_f})}. \quad (13)$$

2. This derivative corresponds to the slope of the curves in Fig. 3 and is a function of the forward normalized current. Therefore, a particular value of this derivative can be used to determine  $I_S$ . For instance, we can measure the values  $I_{F0}$  of the forward current such that the logarithmic derivative is equal to  $-2/3\phi_t(i_f=3)$ . These values ( $I_{F0}$ ) are depicted by the asterisks Fig. 3. Therefore, we can readily calculate  $I_S = I_{F0}/3$ .
3. The pinch-off voltage  $V_P(V_G)$  is also extracted from the common-gate characteristics. Here we assume that the inversion charge density at pinch-off is  $Q'_{IP} = -nC'_{ox}\phi_t$ , which implies that  $i_P=3$ . On the other hand, we adopt for  $V_P$  and  $n$  the definitions

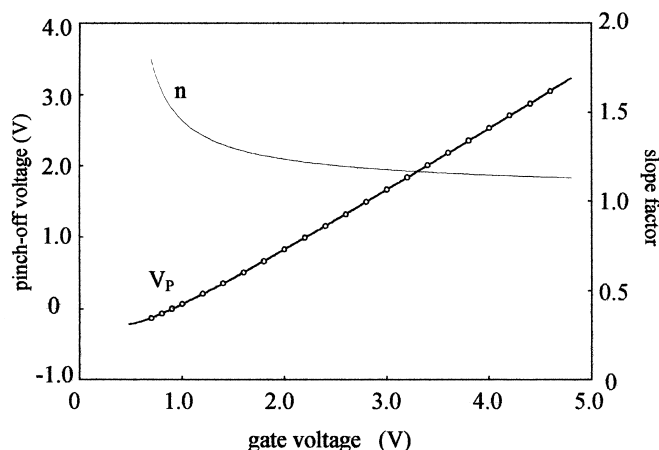


Fig. 4. Pinch-off voltage and slope factor vs. gate voltage for an NMOS transistor with  $t_{ox} = 280 \text{ \AA}$  and  $W = L = 25 \text{ \mu m}$ : (○) extracted values of  $V_P$ ; (—) values of  $V_P$  and  $n$  calculated from theoretical expressions in [4].

in [4]. According to Eq. (12),  $V_P$  is the value of  $V_S$  such that  $I_F = I_S \cdot i_P$ . Adopting,  $i_P = 3$ ,  $V_P$  is equal to  $V_S$  for the asterisks in Fig. 3. Fig. 4 exhibits the extracted and fitted values of the pinch-off voltage, as well as the calculated values of the slope factor. The extraction procedure proposed here is fully independent of the knowledge of transistor dimensions and technological parameters in opposition to the methodology presented in [2].

4. The dependence of the mobility on the electrical transversal field can be extracted from the variations of  $I_S$  and  $n$  with respect to  $V_G$ .

The theoretical and measured ‘common-gate characteristic’ ( $I_D$  vs.  $V_S$  for constant  $V_G$ ) in saturation are shown in Fig. 3 for an NMOS transistor whose oxide thickness ( $t_{ox}$ ) is 280 Å and whose channel dimensions are  $W = L = 25$  μm. The theoretical values have been obtained by using Eq. (12) and agree very well with the experimental results.

## 6. Conclusions

We have presented the physical approximation underlying the Unified Charge Control Model for MOS transistors. We have verified that the UCCM is fully consistent with the basic approximation of the model derived in [3]. Combining the model presented in [3] with the UCCM, we have derived a MOSFET model whose key variables are the forward and reverse

normalized currents. Such a feature is extremely useful, since the bias current has a key role in circuit performance.

## Acknowledgements

The authors would like to thank the financial support of CNPq and CAPES, research agencies of the Brazilian Ministries of Science and Technology and Education, and the ‘Laboratoire de Physique des Composants à Semiconducteur’, Grenoble, for supplying the test devices. The authors are deeply indebted to the anonymous reviewer whose comments certainly contributed to clarify the presentation of this paper.

## References

- [1] Park C-K, Lee C-Y, Lee K, Moon B-J, Byun YH, Shur M. IEEE Trans Electron Dev 1991;ED-38:399.
- [2] Lee K., Shur M., Fjeldly T.A., Ytterdal T. Semiconductor device modeling for VLSI. Englewoods Cliffs: Prentice Hall, 1993.
- [3] Cunha AIA, Schneider MC, Galup-Montoro C. Solid-St Electron 1995;38:1945.
- [4] Enz CC, Krummenacher F, Vittoz EA. Anal Integr Circuits Signal Proc 1995;8:83.
- [5] Tsividis Y. Operation and modeling of the MOS transistor. New York: McGraw-Hill, 1987.